



---

# Synthetic data enables context-aware bioacoustic sound event detection

Benjamin Hoffman<sup>1</sup>, David Robinson<sup>1</sup>, Marius Miron<sup>1</sup>, Vittorio Baglione<sup>2</sup>, Daniela Canestrari<sup>2</sup>, Damian Elias<sup>3</sup>, Eva Trapote<sup>4</sup>, and Olivier Pietquin<sup>1</sup>

<sup>1</sup>Earth Species Project

<sup>2</sup>Universidad de León

<sup>3</sup>University of California Berkeley

<sup>4</sup>Universidad de Valladolid

---

## Abstract

We propose a methodology for training foundation models that enhances their in-context learning capabilities within the domain of bioacoustic signal processing. We use synthetically generated training data, introducing a domain-randomization-based pipeline that constructs diverse acoustic scenes with temporally strong labels. We generate over 8.8 thousand hours of strongly-labeled audio and train a query-by-example, transformer-based model to perform few-shot bioacoustic sound event detection. Our second contribution is a public benchmark of 13 diverse few-shot bioacoustics tasks. Our model outperforms previously published methods by 49%, and we demonstrate that this is due to both model design and data scale. We make our trained model available via an API, to provide ecologists and ethologists with a training-free tool for bioacoustic sound event detection.

## 1 Introduction

Foundation models such as GPT-4 [1] can learn new tasks at inference time from only a handful of labeled examples—a process known as few-shot or in-context learning (ICL) [2]. This property is particularly attractive for application-driven ML domains—like bioacoustics, ecology, and conservation—where domain experts may lack extensive ML training and large labeled datasets [3, 4, 5]. However, while there is a growing push to adapt foundation models for these fields, their success is constrained by data scarcity, which limits the scope of tasks such models can be trained to perform [4].

An example of this situation occurs in few-shot bioacoustic sound event detection (FSBSED), which attempts to provide flexible modeling for the diversity of problems that arise in bioacoustics. In this task, formalized in [6], a model is provided with a *support set*: an audio recording, together with annotations of the onsets and offsets of the first few events of interest. The model must predict onsets and offsets of these events in the *query set*, which is the remainder of the recording. This type of temporally fine-scale detection is required for many applications in animal behavior and ecology [7], however the expertise and time it takes to annotate bioacoustic events has resulted in a lack of data available for training models capable of FSBSED. Prior efforts for FSBSED largely rely on a single 22-hour training dataset described in [6], leading to lightweight models tailored to small-scale data.

Given the diversity of bioacoustic audio and the extreme domain gap between different few-shot detection problems [8], one expects that increasing pre-training data and model size would improve performance. A solution to the lack of a large and diverse training dataset is to construct synthetic acoustic scenes from existing unlabeled audio. This type of data is highly scalable, grants control over data attributes, and, importantly, can be generated to come along with temporally fine-scale annotations [9]. Motivated by this, we ask: Can we train a query-by-example, high-parameter model for FSBSED using only synthetically constructed scenes (Figure 1)?

To generate data, we transform unlabeled raw audio into strongly-labeled scenes using a set of custom preprocessing steps and data augmentations to inject domain randomization into the training process. These are used to train our model, which consists of a lightweight audio encoder and an encoder-only transformer, accepts the entire example at once and directly outputs sound event detection predictions for the unlabeled audio. At inference time, the model learns to make predictions from labeled demonstration audio without fine-tuning, i.e. in-context. To encapsulate the main ideas of our method, we name it DRASDIC: *Domain Randomization for Animal Sound Detection In-Context*.

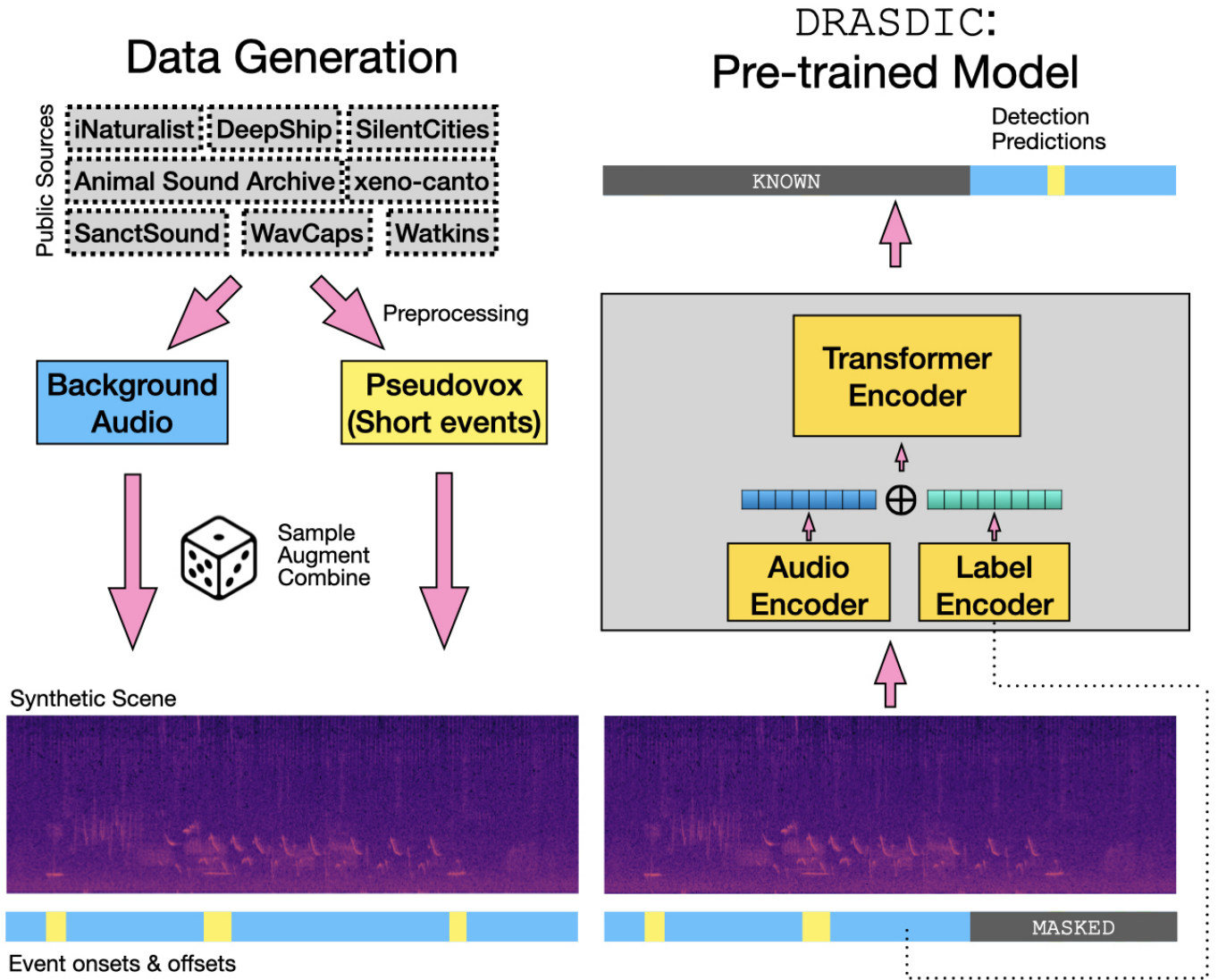


**Figure 1:** We introduce a method for generating synthetic acoustic scenes (Left) and a SotA few-shot detection model (Right).

While we focus on FSBSSED, our proposed data generation method opens the door for foundation models to perform other fine-scale acoustic tasks. As a proof-of-concept, we train a zero-shot detection model (DRASD0S) that is conditioned on only a high-level set of acoustic features such as duration and frequency bounds, which could be provided *a priori* by a researcher familiar with the target sound.

Prior work on FSBSSED has re-used validation data from [8] at test time, because there is no public FSBSSED benchmark. To fill this gap, we developed FASD13: the *Fewshot Animal Sound Detection-13* benchmark. Reserved exclusively for model evaluation, FASD13 complements the validation datasets already in use. FASD13 consists of 13 datasets, each of which includes audio files and annotations of event onsets and offsets (Figure 2, Table 1). They represent a diversity of taxa (birds, insects, arachnids, mammals, amphibians), detection targets (species, call type, life stage), and recording configurations (on-body, passive acoustics, laboratory). Two of these datasets, which focus on on-body recordings of carrion crows and substrate-borne drumming of jumping spiders, have not been released publicly before. The remaining eleven we curate from publicly available sources.

We evaluate DRASDIC on FASD13 and find that it represents a 49% improvement on average over previously published methods. Low-parameter models widely used in the literature are not able to take advantage of the scale of data generated by our method. Our zero-shot method DRASD0S also improves over the current standard approach. These results show that synthetic acoustic scenes can be used to pre-train audio foundation models for bioacoustics tasks which are inaccessible given current data limitations.

In summary, our contributions are: 1) To enable large-scale pretraining for fine-scale bioacoustic tasks, we propose a method for generating synthetic acoustic scenes with temporally-strong labels. 2) We introduce DRASDIC, a state-of-the-art ICL detection model trained using our generated data. 3) We create FASD13, an expansive benchmark for

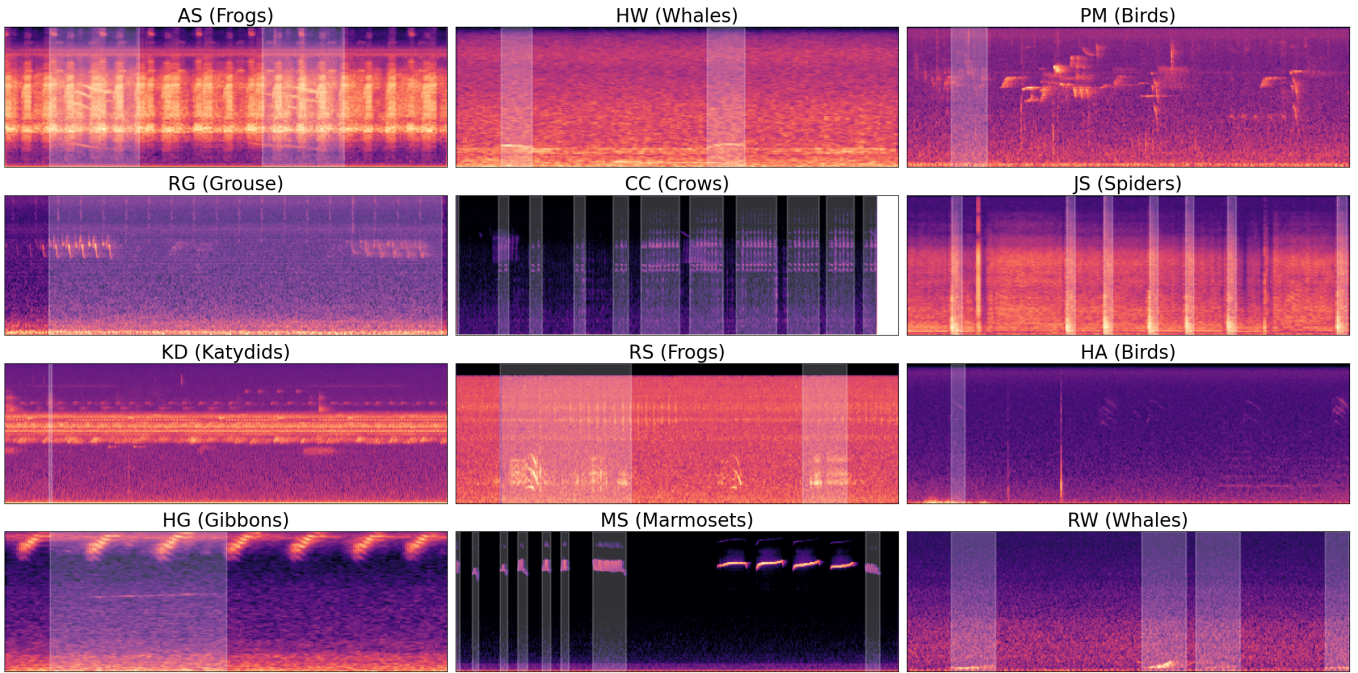


**Figure 2:** We introduce FASD13, an expansive public benchmark for few-shot bioacoustic sound event detection, which includes 13 datasets that represent a diversity of taxa, detection targets, and recording methods. Each spectrogram represents ten seconds of audio; audio from one dataset (GS) is omitted for space. Further details are in Table 1 and the Appendix.

few-shot bioacoustic sound event detection. We make our scene generator, DRASDIC weights and inference API, and benchmark publicly available.<sup>1</sup>

## 2 Related Work

### 2.1 Few-shot sound event detection

Few-shot sound event detection was introduced in [10], and FSBSED in [6]. In bioacoustics, detection problems are highly diverse in terms of detection targets (e.g. a given species, call type, or emotional state), and therefore methods with a fixed ontology (e.g. [11]) do not apply to many situations. Moreover, labeling event onsets and offsets and fine-tuning a model for a specific problem requires expertise and computational resources that may be unavailable to practitioners. Few-shot learning attempts to address both of these challenges. [8] note central challenges in this task include sparse vocalizations, diverse target sounds, dynamic acoustic environments, and domain generalization.

Published approaches include prototypical networks [12], representation learning [13], transductive inference [14, 15]; variations and other methods are described in technical notes submitted as part of the DCASE challenge [16]. In contrast with prior approaches, we adopt a highly parameterized, transformer-based architecture which can model temporal dependencies between sparse events using stacked attention layers. Our method differs from many prior approaches in that it does not rely on fine-tuning at inference time, which can be a potential barrier for the usability of few-shot methods by non-experts.

Previous evaluation campaigns for FSBSED have centered around the DCASE challenge [8]. This challenge historically provided public training and validation datasets, and maintained a private test dataset. Subsequent efforts have either used the public validation set for both model selection and model evaluation [8], or apparently forgone model selection [13]. Our benchmark FASD13 fills this need for public evaluation datasets. In this work, we rely heavily on the validation set from [8] for model selection.

Zero-shot learning—where tasks are specified at inference without examples—has recently emerged in bioacoustics [3, 17, 4]. However, due to data scarcity, no zero-shot model has so far demonstrated temporally fine-grained detection, nor can be prompted with acoustic features. Consequently, the de-facto approach remains the signal processing method BLED [18]. Here, we demonstrate how our synthetic data pipeline addresses this limitation to enable temporally

<sup>1</sup>Available upon publication

fine-grained zero-shot detection in bioacoustics.

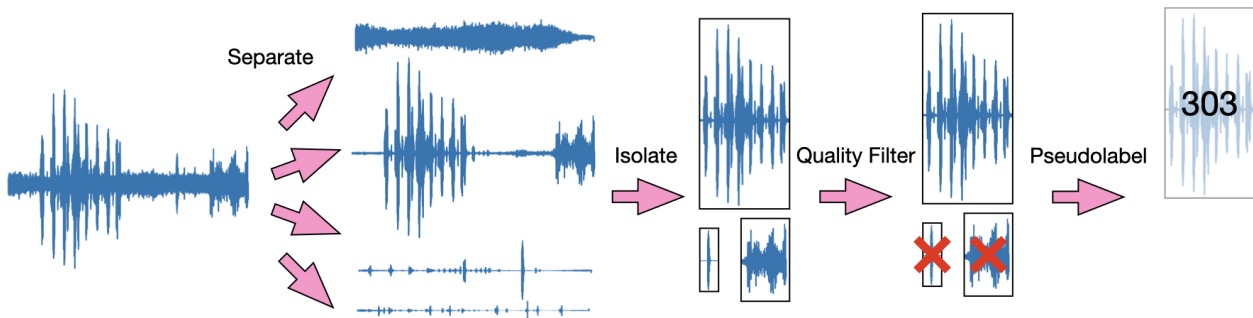
## 2.2 In-context learning

In-context learning (ICL) refers to a model’s ability to perform a task specified through demonstrations at inference time [2]. While originally discussed in the context of language models, in the audio domain, ICL boosts speech translation [19] and text-to-speech synthesis [20]. ICL it has also been extended to fine-scale tasks in computer vision that somewhat resemble FSBSED, which include sementic segmentation [21, 22, 23] and scene understanding [24]. Similar to our method, [22, 23] employ a simple encoder-based architecture.

## 2.3 Synthetic data

Generative vision and audio models have been used to create data for few-shot and low-resource tasks including classification [25], detection [26], representation learning [27], and keyword spotting [28]. We are not aware of a generative audio model that produces high-quality animal sounds, and so instead developed a preprocessing pipeline to isolate potential animal sounds in publicly available data. A similar procedure was developed in [29] in a different context. For sound event detection in general audio, the cut-and-paste-based Scaper [9] library has been used to train models within a fixed ontology [30]. [31] explores the performance impacts of training on a mixture of Scaper’s synthetic acoustic scenes with real data. A challenge of training with synthetic data is that the distribution of the generated data may not match the real-world distribution [32]. Domain randomization, in which attributes of synthetic data are randomized and allowed to take on potentially non-realistic values, has been proposed as a strategy to overcome this domain gap [33]. Prior applications include robotics [34] and computer vision [35].

### Pseudovox Preprocessing



### Scene Generation

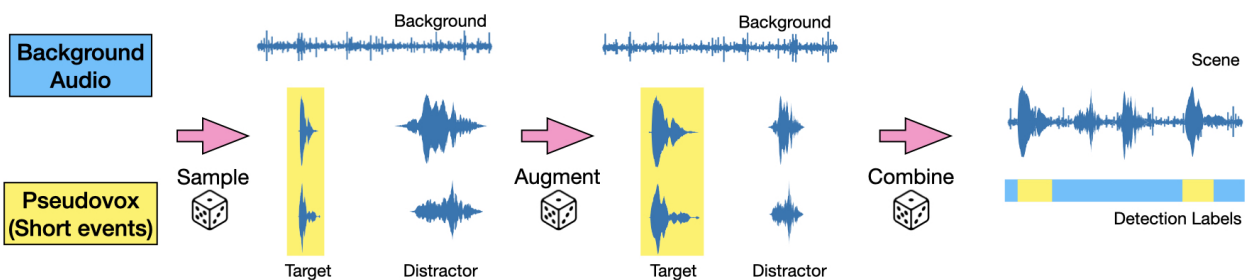


**Figure 3:** Summary of training data preprocessing and scene generation.

## 3 Method

### 3.1 Data Generation

We propose a two-stage approach to generate scenes (Figure 3). Beginning with publicly available unlabeled audio, we assemble a set of background audio tracks (5.1e5 tracks, 5540 hours) and, via extensive preprocessing, a set of short clips containing events dubbed pseudo-vocalizations (or *pseudovox*) (5.4e6 events, 577 hours). These are pseudo-labeled through a clustering step, so that multiple similar-sounding pseudovox can be sampled at one time.



In the second stage, which we perform on-the-fly during model training, clips are randomly sampled from these collections, manipulated with data augmentations, and combined into scenes. Prior work has shown that extensive domain randomization in synthetic data generation improves transfer to real data [33], achieving the same result as strong regularization or data augmentation. Similarly, our generated scenes may be outside of what is usually recorded in the real world, due to preprocessing steps and randomness in the scene generation process. We view this as a way of increasing test-time robustness of our method.

**Preprocessing** To construct our collection of pseudovox, we obtained publicly available raw audio recordings from iNaturalist [36], Animal Sound Archive [37], xeno-canto [38], Watkins [39], and WavCaps [40]. To remove background noise, we separated each recording into four stems using BirdMixIT [41]. For each stem, we isolated potential pseudovox: segments where the amplitude envelope exceeded 25% of the maximum amplitude of the raw recording, indicating that some acoustic event was potentially occurring. There remained a high proportion of these segments that included no clear acoustic event, so we performed a quality filtering step. For this, we obtained the final activations from BirdNET [11], applied to each segment. BirdNET is a bird sound classification model whose clip-level audio representations have been shown to be useful for other bioacoustics tasks [42]. Using manual annotations of segment quality, we trained a binary linear classifier on the corresponding BirdNET embeddings. We applied this quality filter to the potential pseudovox; those that passed the filter became the final collection of pseudovox. This procedure resulted in  $M = 5.4e6$  pseudovox. Finally, to obtain pseudolabels for the pseudovox, we applied  $k$ -means clustering to the pseudovox’s BirdNET activations. We did this for  $k \in K = \{\lfloor M/128 \rfloor, \lfloor M/64 \rfloor, \lfloor M/32 \rfloor, \lfloor M/16 \rfloor, \lfloor M/8 \rfloor\}$ , to obtain different levels of cluster homogeneity. For background audio, we took the raw recordings above, along with recordings from SilentCities [43], DeepShip [44], and SanctSound [45].

**Scene Generation** Scene generation consists of three parts: sampling audio clips, manipulating them with data augmentations, and combining them to form a scene. In Section 5.6, we investigate how the randomness in this process influences model performance.

We first sample two background tracks which are overlaid on each other. We choose a clustering level  $k \in K$  and two clusters  $c_T, c_D$  from the clusters of level  $k$ . We sample a random number of target pseudovox from  $c_T$ , and a random number of distractor pseudovox from  $c_D$ . We apply reverb, resampling, time flipping, and amplitude augmentations to pseudovox, and resampling augmentations to background tracks. We paste pseudovox into the background track, one-by-one, with a random time gap between pseudovox.

We maintain a binary annotation mask for the scene. This mask is initialized with zeros, and changed to ones where target pseudovox are added. Distractor pseudovox do not change the mask; they join whatever sounds are already present in the background tracks. To generate one training example, two scenes (support and query) are generated, drawing pseudovox from the same  $c_T, c_D$  for both. With some probability, the background tracks of the query are chosen to be different than those of the support.

## 3.2 Model

Using our synthetic scenes, we train our transformer-based model DRASDIC. During training the model is presented with annotated support audio and unannotated query audio, and must predict the detection labels for the query audio.

**Architecture** To emphasize the contribution of the data scale provided by our scene generation method, and noting that encoder-only architectures have been used successfully for fine-scale ICL problems in computer vision [22], we adopt a straightforward but highly parametrized BERT-like architecture. This is preceded by a simple CNN spectrogram encoder. In initial experiments we used AVES [46], which was pre-trained on animal sounds, as a frozen audio encoder. The resulting models performed poorly on the DCASE validation set [8], in particular for long-duration events. Performance on the validation set increased with a CNN encoder.

In detail, for DRASDIC support and query audio is resampled to 16 kHz, concatenated, and converted to a log mel-spectrogram (256 mels, hop size 160). The CNN encoder consists of a convolutional block followed by two residual blocks [47] (kernel sizes 7, 3, 3, hidden size 64). Mean pooling in the vertical (frequency) axis is applied after each block with kernel size 2. The frequency and hidden dimensions of outputs are flattened to one dimension and mean-pooled with kernel size 2. The final frame rate is 50 Hz. The binary support label mask is max-pooled to 50 Hz, passed through a learned per-frame label encoding, and added to the CNN outputs of the support audio. This label-enriched audio representation is fed into a transformer encoder (hidden size 768, depth 12, 12 heads) with rotary

position encoding [48], flash attention [49], and SwiGLU activations [50]. A final linear layer converts each output frame into detection logits.

DRASD $\emptyset$ S modifies this approach by replacing the support audio encoder with a feature encoder (MLP with one hidden layer of size 100, output size 768). Input features are five numbers: the typical peak frequency, high frequency, low frequency, duration, and signal-to-noise ratio (SNR) of the target event. The encoded features are concatenated with the encoded query audio and passed to the transformer.

**Training** Both DRASDIC and DRASD $\emptyset$ S were randomly initialized and trained with per-frame binary cross-entropy loss on the query labels, using AdamW [51] with  $(\beta_0, \beta_1) = (0.9, 0.999)$  and weight decay 0.01. DRASDIC is trained on support-query pairs of total duration  $\text{dur}_s + \text{dur}_q$  seconds. Based on initial experiments, we found that a long  $\text{dur}_s$  improved validation performance. For DRASDIC we set  $\text{dur}_s = 30$  and for both DRASDIC and DRASD $\emptyset$ S we set  $\text{dur}_q = 10$ ; see also Section 5.6.

Model, data generation, and training hyperparameters were chosen through random search. As our model selection criterion, we used average performance on the validation datasets from [8]. Inspired by [52], we applied curriculum learning to gradually increase task difficulty during training. This linearly decays the minimum pseudovox SNR from 0 dB to a minimum of -20 dB for an initial  $5e4$  steps (DRASD $\emptyset$ S:  $3e4$  steps). The learning rate is linearly increased for  $1e4$  steps to a maximum of  $2e-5$ , and then decayed to 0 after  $1e5$  steps (cosine schedule) using batch size of 8 (DRASD $\emptyset$ S: 4). Parameters governing data generation are provided in the Appendix. Audio features for DRASD $\emptyset$ S are computed during training, based on the mean power spectrum of target pseudovox. Models were implemented in PyTorch [53].

## 4 Public Benchmark

**Table 1:** Details of FASD13. Additional details are in the Appendix. Datasets with a  $\dagger$  are presented for the first time here. Terrestrial and underwater autonomous passive acoustic monitoring devices are abbreviated T. PAM and U. PAM, respectively.

Dataset	Full Name	N files	Dur (hr)	N events	Recording type	Location	Taxa	Detection target
AS [54]	AnuraSet	12	0.20	162	T. PAM	Brazil	Anura	Species
CC $\dagger$	Carrion Crow	10	10.00	2200	On-body	Spain	Corvus corone + Clamator glandarius	Species + Life Stage
GS [55]	Gunshot	7	38.33	85	T. PAM	Gabon	Homo sapiens	Production Mechanism
HA [56]	Hawaiian Birds	12	1.10	628	T. PAM	Hawaii, USA	Aves	Species
HG [57]	Hainan Gibbon	9	72.00	483	T. PAM	Hainan, China	Nomascus hainanus	Species
HW [58]	Humpback Whale	10	2.79	1565	U. PAM	North Pacific Ocean	Megaptera novaeangliae	Species
JS $\dagger$	Jumping Spider	4	0.23	924	Substrate	Laboratory	Habronattus	Sound Type
KD [59]	Katydid	12	2.00	883	T. PAM	Panamá	Tettigoniidae	Species
MS [60]	Marmoset	10	1.67	1369	Laboratory	Laboratory	Callithrix jacchus	Vocalization Type
PM [61]	Powdermill	4	6.42	2032	T. PAM	Pennsylvania, USA	Passeriformes	Species
RG [62]	Ruffed Grouse	2	1.50	34	T. PAM	Pennsylvania, USA	Bonasa umbellus	Species
RS [63]	Rana Sierrae	7	1.87	552	U. PAM	California, USA	Rana sierrae	Species
RW [64]	Right Whale	10	5.00	398	U. PAM	Gulf of St. Lawrence	Eubalaena glacialis	Species

A collection of public FSBSED datasets was previously provided in [6, 8], but these were designated as datasets for model development (i.e. training and validation). We complement these with FASD13, a public benchmark to be used for model evaluation (Figure 2, Table 1). FASD13 consists of 13 bioacoustics datasets, each of which includes between 2 and 12 recordings. Eleven of these datasets were used from previous studies; they were chosen for their taxonomic diversity, varied recording conditions, and quality of their annotations. Two (CC and JS) are presented here for the first time. All datasets were developed alongside studies of ecology or animal behavior, and represent a range of realistic problems encountered in bioacoustics data. Details of dataset collection and preprocessing steps are in the Appendix.

We follow the data format in [6]: Each recording comes with annotations of the onsets and offsets of *positive* sound events, i.e. sounds coming from a predetermined category (such as a species label or call type). An  $N$ -shot detection system is provided with the audio up through the  $N^{\text{th}}$  positive event, and must predict the onsets and offsets of positive events in the rest of the recording.

We provide two versions of each recording in FASD13: the *within-file version*, in which the support and query audio come from the same original recording, and the *cross-file version*. In the cross-file version, which is tailored to a 5-shot problem, the support set comes from a different recording than the query set. In more detail: Each recording in the within-file version has labels associated with one class (e.g. species label). Each class appears in more than

**Table 2:** F1 scores @0.3 IoU on FASD13. Methods marked with † were pre-trained using our generated data, rather than the data used in the original publication. Methods marked with \* involve no gradient updates at inference time.

5-shot, within-recording														
Model	AS	CC	GS	HA	HG	HW	JS	KD	MS	PM	RG	RS	RW	Avg
BEATS+linear	.350	.003	.056	.093	<b>.242</b>	.173	.028	.049	.462	.212	<b>.732</b>	.007	.316	.209
Protonet*	.356	.189	.156	.239	.038	.085	.136	.316	.590	.260	.000	.216	.393	.229
Protonet†*	.305	.224	.151	.307	.023	.116	.166	.418	.536	.235	.121	.195	.342	.242
Transductive	.299	.144	.002	.283	.020	.116	.279	.218	.569	.159	.089	.169	.048	.184
SCL*	.516	.333	.025	.438	.010	.255	.281	.263	.402	.237	.049	.219	.509	.272
SCL+finetuning	.565	<b>.341</b>	.017	.467	.008	.382	<b>.302</b>	.381	.476	.327	.042	.285	.275	.298
SCL†*	.545	.287	.024	.433	.008	.393	.243	.207	.429	.336	.038	.218	.228	.261
SCL†+finetuning	.571	.205	.030	.479	.005	<b>.453</b>	.132	.220	.516	.450	.050	.292	.223	.279
DRASDIC †* (ours)	<b>.645</b>	.272	<b>.593</b>	<b>.587</b>	.144	.337	.099	<b>.644</b>	<b>.783</b>	<b>.474</b>	.092	<b>.352</b>	<b>.764</b>	<b>.445</b>
5-shot, cross-recording														
Model	AS	CC	GS	HA	HG	HW	JS	KD	MS	PM	RG	RS	RW	Avg
BEATS+linear	.114	.000	.139	.085	.063	.007	.002	.004	.349	.068	<b>.605</b>	.082	.133	.127
Protonet*	.404	.063	.084	.150	.025	.124	.132	.143	.570	.204	.000	.168	.281	.181
Protonet†*	.255	.070	.100	.287	.012	.119	.084	.013	.413	.262	.000	.212	.228	.176
Transductive	.042	.082	.001	.212	.015	.127	<b>.352</b>	.184	.536	.101	.108	.189	.043	.153
SCL*	.442	.157	.026	.254	.002	<b>.218</b>	.078	.155	.366	.216	.048	.263	.458	.207
SCL+finetuning	.397	.187	.016	.344	.003	.170	.174	.178	.415	.340	.084	.331	.197	.218
SCL†*	.469	<b>.238</b>	.032	.329	.005	.184	.169	.098	.437	.417	.044	.302	.193	.224
SCL†+finetuning	.408	.167	.037	<b>.352</b>	.005	.124	.193	.111	.461	<b>.447</b>	.096	.353	.209	.228
DRASDIC †* (ours)	<b>.500</b>	.031	<b>.641</b>	.321	<b>.091</b>	.145	.004	<b>.544</b>	<b>.650</b>	.407	.058	<b>.367</b>	<b>.689</b>	<b>.342</b>
0-shot														
Model	AS	CC	GS	HA	HG	HW	JS	KD	MS	PM	RG	RS	RW	Avg
BLED*	<b>.505</b>	.067	.138	.209	.060	.209	<b>.739</b>	.417	.518	.302	<b>.338</b>	.160	.177	.295
DRASDØS †* (ours)	.163	<b>.130</b>	<b>.259</b>	<b>.340</b>	<b>.116</b>	<b>.493</b>	.000	<b>.497</b>	<b>.549</b>	<b>.428</b>	.082	<b>.246</b>	<b>.645</b>	<b>.304</b>

one recording. We cut each recording after  $N = 5$  positive events to divide the support and query sets. Within each class label, we shuffled and re-paired the support sets and query sets. Compared to the within-file version, this version represents a harder detection problem requiring greater generalization between support and query (Appendix Figure 8).

## 5 Experimental Evaluation

We evaluate models based on their ability to detect events after the fifth positive event in each recording of FASD13. Few-shot models (DRASDIC and its comparisons) have access to the audio and annotations up to the fifth positive event. Zero-shot methods use only high level features (the typical duration, high- and low-frequency, peak frequency, and SNR of target events). To set the value of the input features we measured these features on the first five positive events in a recording and took the median. Results for the validation set are in the Appendix. For all methods, we used validation set performance as the model selection criterion and only evaluated one final model version on FASD13.

### 5.1 Inference

For DRASDIC, for each of the five positive events in the support set, we take the  $\text{dur}_s$ -seconds of labeled audio surrounding that event; this plus a  $\text{dur}_q$ -second window of unlabeled audio forms one DRASDIC input. We average the detection logits for the unlabeled audio coming from all five of the inputs constructed this way. This is repeated for  $\text{dur}_q$ -second windows across the entire query set. Inference with DRASDØS uses one forward pass through per query window. For both models, frames with predicted detection probability above a fixed threshold of 0.5 become positive detections. These are smoothed: detections separated by a gap of  $\min(1, d/2)$  seconds are merged, and then detections lasting less than  $\min(1/2, d/2)$  seconds are discarded. Here  $d$  is the duration of the shortest event in the support set.

## 5.2 Metrics

Following [6], we evaluate models based on per-dataset detection F1. First, model detections are matched with annotated events. Detections and annotations with  $\geq 0.3$  intersection-over-union (IoU) are identified as potential matches. Each detection is then assigned to at most one annotation, and vice-versa, using a graph matching algorithm [65]. Paired detections are true positives, unpaired detections are false positives, and unpaired annotations are false negatives.

## 5.3 Comparison methods

We compare DRASDIC with essentially all of the previously published methods we are aware of for FSBSSED that contain publicly available implementations. The first, “BEATS+linear” is a simple supervised baseline which consists of a frozen BEATS encoder [66] and a final linear layer. Support audio is windowed (4 seconds, 50% overlap) and the final layer is trained for 100 epochs using cross-entropy loss. The initial learning rate of 0.01 (tuned using the validation set) is decayed to 0 using a cosine schedule. “Protonet” is the prototypical network from [8], which itself adapts [12]. “Transductive” [14] uses a CNN encoder that is updated using unlabeled audio from the query set. “SCL” applies the supervised contrastive learning method introduced by [13]. “SCL+finetuning”, also introduced by [13] extends this by using support audio to fine-tune the encoder that was pre-trained using the SCL method.

For Protonet, SCL, and SCL+Finetuning, we train a version using the standard data from [6]. We also train a version using our generated scenes (5e4 scenes, each 40 seconds), which represents a  $25\times$  increase in data quantity over the data used for training the original models.

We compare DRASDØS with a band-limited energy detector (BLED), which is the only widely-used method we are aware of that performs zero-shot bioacoustic sound event detection based on high-level acoustic features. BLED detects events based on their within-band energy relative to a recording’s noise floor, and is included in Raven Pro, a standard software package used by bioacousticians [18]. Similar to DRASDØS, it requires the user to specify a target event’s frequency bounds, within-band SNR, and duration. For our experiments, we re-implemented BLED based on the Raven Pro documentation and tuned the detection threshold using the validation set. Detections produced by BEATS+Linear and BLED are smoothed in the same way as DRASDIC and DRASDØS.

## 5.4 Few-shot experiments

We compare model performance on FASD13 (Table 2). For DRASDIC and DRASDØS, some datasets (JS, KD, MS, PB, PB24) contain events that are above the models’ 8kHz Nyquist frequency, or that are brief relative to the models’ 50Hz frame rate. For these, we give the model a 1/2-slowed version (1/6 for KD). For a fair comparison, we give other methods *both* the slowed and full-speed version of the data, and keep the version with the better score.

On the within-file version of FASD13, DRASDIC outperforms all the alternatives on 8 out of 13 datasets. Across datasets DRASDIC has an average F1 score of .147 over the next best model (49% improvement). For the cross-file version of FASD13, DRASDIC outperforms all others on 7 of 13 datasets and improves on the next best model by .114 F1 on average (50% improvement). The cross-file version is more difficult on average for all models; for DRASDIC the performance drops on average by .103 F1.

Qualitatively, DRASDIC can detect a variety of target sounds, even in the presence of other sounds occupying the same frequency bands (Figure 4, top). Performance is strong across a variety of taxa and conditions. A failure case is for the JS dataset, which consists of jumping spider drumming. Here, the detection targets are specific drum types, and distinguishing between drum types relies partly on the rate of drumming. Our scene generator did not account for this type of information, but could be adapted to do so in the future. Other failure cases are in Figure 4, bottom.

For the comparison methods we trained with our generated data, there was no clear performance increase. These methods, which adopt a CNN architecture, have fewer than 1/10 the trainable parameters as DRASDIC, and likely do not have the capacity to take advantage of increased data scale.

## 5.5 Zero-shot experiments

Compared with BLED, DRASDØS performs better on 10 of 13 datasets in FASD13 (Table 2, bottom). Average performance is minorly better (.009 F1), but much of the contribution to the average F1 for BLED comes from its high performance on JS and AS. Compared with DRASDIC, DRASDØS performed worse with the exception of HW. It is possible that the additional information of high- and low-frequency bounds, which were not included in DRASDIC inputs, allowed DRASDØS to better locate low SNR vocalizations.



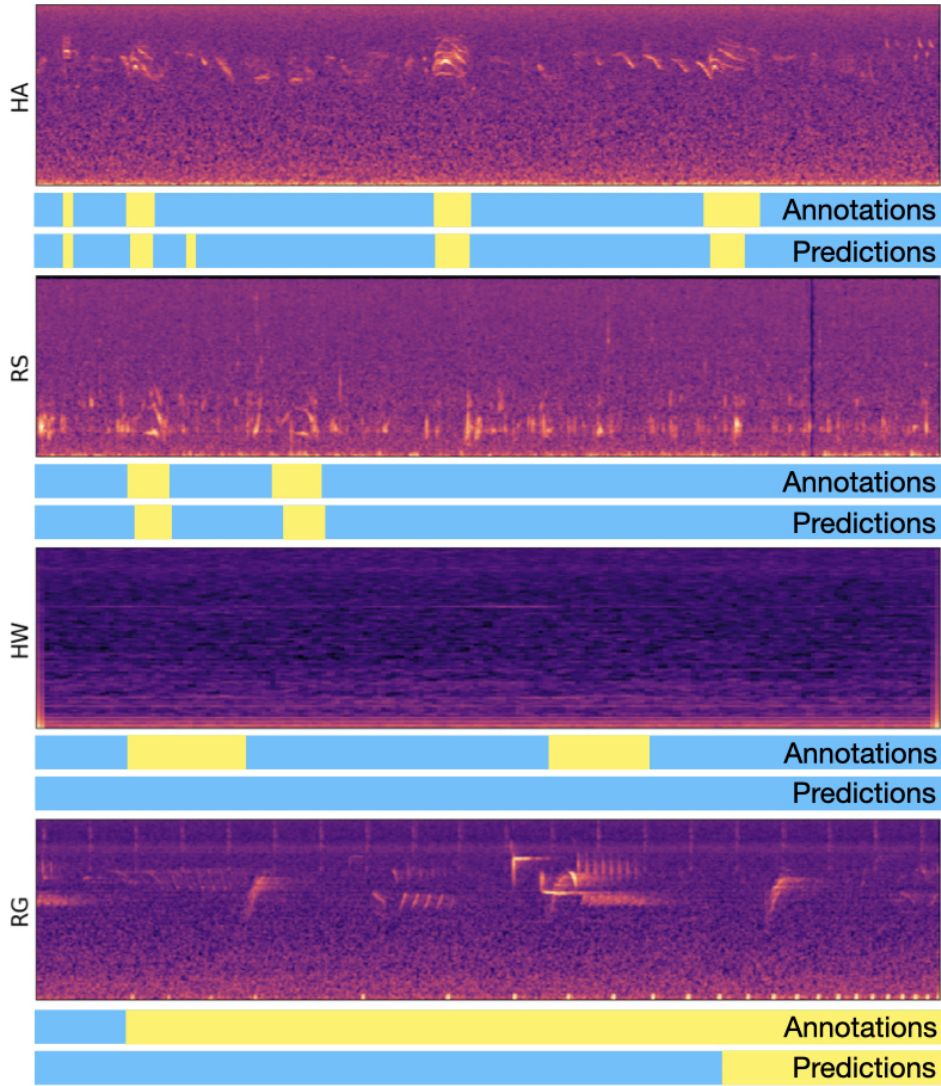


**Figure 4:** Qualitative results for few-shot task; events are in yellow. DRASDIC detects target sounds in dynamic environments (top two), but challenges include extremely low SNR (third), and the extended low-frequency drumming displays of ruffed grouse (bottom). Each spectrogram represents 10 seconds of audio.

## 5.6 Additional experiments

We investigated the impacts of adjusting the randomness governing our scene generation procedure (Table 3). We perturbed the level of homogeneity of target events in a scene, the typical rate of events, the loudness of events, and whether we apply pitch shifting augmentations (details in Appendix). Average performance is stable across some of these perturbations, but decreases when the randomness in event rate and event SNR is decreased. These parameters likely influence the level of diversity present across generated scenes more than the others.

Eliminating random pitch shifts resulted in slightly better performance on FASD13. Designing a domain randomization strategy is an optimization problem [32], which we approached through a model selection criterion. This criterion did not produce the best model on the test set, aligning with the observation [8] that strong domain shifts between few-shot tasks present a challenge for FSBSSED model development.

We performed ablations on our modeling and training approach (Table 3, bottom). Performance decreased when  $\text{dur}_s$  was reduced to 10 seconds. It also decreased when we removed the transformer and trained the remaining CNN audio encoder with a per-frame prototypical loss [67], a commonly adopted strategy for FSBSSED [16]. Removing curriculum learning decreased validation performance but not performance on FASD13.

Finally, we investigated the effect of reducing the amount of training data available. We trained models with total duration of generated data equal to the duration of the train set adopted by other methods ( $\approx 22$  hours), and also with  $10\times$  this amount. These performed poorly on FASD13.

**Table 3:** Average F1 scores @0.3 IoU on FASD13 and validation datasets. All results are for our model (DRASDIC) trained with different data generation hyperparameters (top) or training/model ablations (bottom).

Data modification	Avg (within)	Avg (cross)	Avg (val)
Reference	.445	.342	<b>.704</b>
High homogeneity in events	.429	.344	.630
Low homogeneity in events	.444	.336	.606
High events / second	.381	.292	.437
Low events / second	.370	.298	.669
Only high SNR events	.402	.300	.620
Only low SNR events	.438	.333	.682
No pitch/time shifting	<b>.457</b>	<b>.376</b>	.613
Ablation	Avg (within)	Avg (cross)	Avg (val)
Reference	<b>.445</b>	.342	<b>.704</b>
No curriculum learning	.441	<b>.362</b>	.644
Shorter support (10 s)	.406	.324	.618
No transformer	.354	.261	.550
Reduced data (22 h)	.130	.108	.088
Reduced data (220 h)	.354	.253	.504

## Conclusion

To provide a training-free solution for fine-scale bioacoustic sound event detection, we develop a ICL transformer model DRASDIC. We develop a domain-randomization based data-generation pipeline, and train our model on over 8.8 thousand hours of synthetic acoustic scenes. We additionally provide FASD13, a new benchmark for few-shot bioacoustic sound event detection. Our model substantially improves upon previous state-of-the-art. We demonstrate that these improvements are due to both our modeling approach and the data scale provided by our scene generation method.

## References

- [1] OpenAI, Achiam J, Adler S, Agarwal S, Ahmad L, Akkaya I, et al.. GPT-4 Technical Report; 2024. Available from: <https://arxiv.org/abs/2303.08774>.
- [2] Brown T, Mann B, Ryder N, Subbiah M, Kaplan JD, Dhariwal P, et al. Language Models are Few-Shot Learners. In: Larochelle H, Ranzato M, Hadsell R, Balcan MF, Lin H, editors. Advances in Neural Information Processing Systems. vol. 33; 2020. p. 1877-901.
- [3] Robinson D, Miron M, Hagiwara M, Pietquin O. NatureLM-audio: an Audio-Language Foundation Model for Bioacoustics; 2024. Available from: <https://arxiv.org/abs/2411.07186>.
- [4] Miao Z, Zhang Y, Fabian Z, Hernandez Celis A, Beery S, Li C, et al. New frontiers in AI for biodiversity research and conservation with multimodal language models. Preprint. 2024. Available from: <https://doi.org/10.32942/X22S6F>.
- [5] Fabian Z, Miao Z, Li C, Zhang Y, Liu Z, Hernández A, et al.. Multimodal Foundation Models for Zero-shot Animal Species Recognition in Camera Trap Images; 2023. Available from: <https://arxiv.org/abs/2311.01064>.
- [6] Nolasco I, Singh S, Morfi V, Lostanlen V, Strandburg-Peshkin A, Vidaña-Vila E, et al. Learning to detect an animal sound from five examples. Ecological Informatics. 2023;77:102258. Available from: <https://www.sciencedirect.com/science/article/pii/S157495412300287X>.

- [7] Stowell D. Computational bioacoustics with deep learning: a review and roadmap. *PeerJ*. 2022;10:e13152. Available from: <https://europepmc.org/articles/PMC8944344>.
- [8] Liang J, Nolasco I, Ghani B, Phan H, Benetos E, Stowell D. Mind the Domain Gap: a Systematic Analysis on Bioacoustic Sound Event Detection; 2024. Available from: <https://arxiv.org/abs/2403.18638>.
- [9] Salamon J, MacConnell D, Cartwright M, Li P, Bello JP. Scaper: A library for soundscape synthesis and augmentation. In: 2017 IEEE Workshop on Applications of Signal Processing to Audio and Acoustics (WASPAA); 2017. p. 344-8.
- [10] Wang Y, Salamon J, Bryan NJ, Bello JP. Few-shot sound event detection. In: ICASSP 2020-2020 IEEE International Conference on Acoustics, Speech and Signal Processing (ICASSP). IEEE; 2020. p. 81-5.
- [11] Kahl S, Wood CM, Eibl M, Klinck H. BirdNET: A deep learning solution for avian diversity monitoring. *Ecological Informatics*. 2021;61:101236.
- [12] Liu H, Liu X, Mei X, Kong Q, Wang W, Plumbley MD. SEGMENT-LEVEL METRIC LEARNING FOR FEW-SHOT BIOACOUSTIC EVENT DETECTION. *DCASE*. 2022.
- [13] Moummad I, Farrugia N, Serizel R. Regularized Contrastive Pre-Training for Few-Shot Bioacoustic Sound Detection. In: ICASSP 2024 - 2024 IEEE International Conference on Acoustics, Speech and Signal Processing (ICASSP); 2024. p. 1436-40.
- [14] Yang D, Wang H, Zou Y, Ye Z, Wang W. A Mutual Learning Framework for Few-Shot Sound Event Detection. In: ICASSP 2022 - 2022 IEEE International Conference on Acoustics, Speech and Signal Processing (ICASSP); 2022. p. 811-5.
- [15] You L, Coyotl EP, Gunturu S, Van Segbroeck M. Transformer-Based Bioacoustic Sound Event Detection on Few-Shot Learning Tasks. In: ICASSP 2023 - 2023 IEEE International Conference on Acoustics, Speech and Signal Processing (ICASSP); 2023. p. 1-5.
- [16] Nolasco I, Singh S, Vidana-Villa E, Grout E, Morford J, Emmerson M, et al. Few-shot bioacoustic event detection at the dcase 2022 challenge. *arXiv preprint arXiv:220707911*. 2022.
- [17] Robinson D, Robinson A, Akrapongpisak L. Transferable Models for Bioacoustics with Human Language Supervision. In: IEEE International Conference on Acoustics, Speech and Signal Processing, ICASSP 2024, Seoul, Republic of Korea, April 14-19, 2024. IEEE; 2024. p. 1316-20. Available from: <https://doi.org/10.1109/ICASSP48485.2024.10447250>.
- [18] Cornell Lab of Ornithology. Raven Pro: Interactive Sound Analysis Software; 2024.
- [19] Chen Z, Huang H, Andrusenko AY, Hrinchuk O, Puvvada KC, Li J, et al. SALM: Speech-Augmented Language Model with in-Context Learning for Speech Recognition and Translation. *ICASSP 2024 - 2024 IEEE International Conference on Acoustics, Speech and Signal Processing (ICASSP)*. 2023:13521-5. Available from: <https://api.semanticscholar.org/CorpusID:264146423>.
- [20] Le M, Vyas A, Shi B, Karrer B, Sari L, Moritz R, et al. Voicebox: Text-Guided Multilingual Universal Speech Generation at Scale. In: *Advances in Neural Information Processing Systems*. vol. 36; 2023. p. 14005-34.
- [21] Bar A, Gandelsman Y, Darrell T, Globerson A, Efros AA. Visual Prompting via Image Inpainting; 2022. Available from: <https://arxiv.org/abs/2209.00647>.
- [22] Wang X, Zhang X, Cao Y, Wang W, Shen C, Huang T. SegGPT: Towards Segmenting Everything in Context. In: *Proceedings of the IEEE/CVF International Conference on Computer Vision (ICCV)*; 2023. p. 1130-40.
- [23] Wang X, Wang W, Cao Y, Shen C, Huang T. Images Speak in Images: A Generalist Painter for In-Context Visual Learning. In: *Proceedings of the IEEE/CVF Conference on Computer Vision and Pattern Recognition (CVPR)*; 2023. p. 6830-9.

- [24] Balazevic I, Steiner D, Parthasarathy N, Arandjelović R, Henaff O. Towards In-context Scene Understanding. In: *Advances in Neural Information Processing Systems*. vol. 36; 2023. p. 63758-78.
- [25] He R, Sun S, Yu X, Xue C, Zhang W, Torr P, et al.. Is synthetic data from generative models ready for image recognition?; 2023. Available from: <https://arxiv.org/abs/2210.07574>.
- [26] Lin S, Wang K, Zeng X, Zhao R. Explore the Power of Synthetic Data on Few-shot Object Detection; 2023. Available from: <https://arxiv.org/abs/2303.13221>.
- [27] Tian Y, Fan L, Isola P, Chang H, Krishnan D. StableRep: Synthetic Images from Text-to-Image Models Make Strong Visual Representation Learners. In: Oh A, Naumann T, Globerson A, Saenko K, Hardt M, Levine S, editors. *Advances in Neural Information Processing Systems*. vol. 36. Curran Associates, Inc.; 2023. p. 48382-402.
- [28] Zhu P, Agarwal D, Bartel JW, Partridge K, Park HJ, Wang Q. Synth4Kws: Synthesized Speech for User Defined Keyword Spotting in Low Resource Environments. In: *Proc. SynData4GenAI 2024*; 2024. p. 11-5.
- [29] Michaud F, Sueur J, Le Cesne M, Hauptert S. Unsupervised classification to improve the quality of a bird song recording dataset. *Ecological Informatics*. 2023;74:101952. Available from: <https://www.sciencedirect.com/science/article/pii/S1574954122004022>.
- [30] Serizel R, Turpault N, Shah A, Salamon J. Sound Event Detection in Synthetic Domestic Environments. In: *ICASSP 2020 - 2020 IEEE International Conference on Acoustics, Speech and Signal Processing (ICASSP)*; 2020. p. 86-90.
- [31] Turpault N, Serizel R. Training Sound Event Detection On A Heterogeneous Dataset; 2020. Available from: <https://arxiv.org/abs/2007.03931>.
- [32] Chen X, Hu J, Jin C, Li L, Wang L. Understanding Domain Randomization for Sim-to-real Transfer. In: *International Conference on Learning Representations*; 2022. Available from: <https://openreview.net/forum?id=T8vZHIRTrY>.
- [33] Tobin J, Fong R, Ray A, Schneider J, Zaremba W, Abbeel P. Domain randomization for transferring deep neural networks from simulation to the real world. *2017 IEEE/RSJ International Conference on Intelligent Robots and Systems (IROS)*. 2017:23-30. Available from: <https://api.semanticscholar.org/CorpusID:2413610>.
- [34] Peng XB, Andrychowicz M, Zaremba W, Abbeel P. Sim-to-Real Transfer of Robotic Control with Dynamics Randomization. *2018 IEEE International Conference on Robotics and Automation (ICRA)*. 2017:1-8. Available from: <https://api.semanticscholar.org/CorpusID:3707478>.
- [35] Tremblay J, Prakash A, Acuna D, Brophy M, Jampani V, Anil C, et al. Training Deep Networks with Synthetic Data: Bridging the Reality Gap by Domain Randomization. *2018 IEEE/CVF Conference on Computer Vision and Pattern Recognition Workshops (CVPRW)*. 2018:1082-10828. Available from: <https://api.semanticscholar.org/CorpusID:4929980>.
- [36] iNaturalist;. Accessed 2023-05-01. <https://www.inaturalist.org/>. Available from: <https://www.inaturalist.org/>.
- [37] Museum für Naturkunde Berlin. Animal Sound Archive;. Accessed via gbif.org 2023-05-09. <https://doi.org/10.15468/0bpa1r>.
- [38] Xeno-canto: Bird sounds from around the world;. Accessed 2023-05-15. <https://www.xeno-canto.org/>. Available from: <https://www.xeno-canto.org/>.
- [39] Sayigh L, Daher MA, Allen J, Gordon H, Joyce K, Stuhlmann C, et al. The Watkins Marine Mammal Sound Database: An online, freely accessible resource. *Proceedings of Meetings on Acoustics*. 2016;27(1):040013. Available from: <https://asa.scitation.org/doi/abs/10.1121/2.0000358>.
- [40] Mei X, Meng C, Liu H, Kong Q, Ko T, Zhao C, et al. WavCaps: A ChatGPT-Assisted Weakly-Labelled Audio Captioning Dataset for Audio-Language Multimodal Research. *arXiv*. 2023.

- [41] Denton T, Wisdom S, Hershey JR. Improving bird classification with unsupervised sound separation. In: ICASSP 2022-2022 IEEE International Conference on Acoustics, Speech and Signal Processing (ICASSP). IEEE; 2022. p. 636-40.
- [42] Ghani B, Denton T, Kahl S, et al. Global birdsong embeddings enable superior transfer learning for bioacoustic classification. *Scientific Reports*. 2023;13:22876. Available from: <https://doi.org/10.1038/s41598-023-49989-z>.
- [43] Challéat S, Farrugia N, Froidevaux JSP, et al. A dataset of acoustic measurements from soundscapes collected worldwide during the COVID-19 pandemic. *Scientific Data*. 2024;11:928. Available from: <https://doi.org/10.1038/s41597-024-03611-7>.
- [44] Irfan M, Jiangbin Z, Ali S, Iqbal M, Masood Z, Hamid U. DeepShip: An underwater acoustic benchmark dataset and a separable convolution based autoencoder for classification. *Expert Systems with Applications*. 2021;183:115270.
- [45] NOAA. Passive Acoustic Data Collection; 2017.
- [46] Hagiwara M. Aves: Animal vocalization encoder based on self-supervision. In: ICASSP 2023-2023 IEEE International Conference on Acoustics, Speech and Signal Processing (ICASSP). IEEE; 2023. p. 1-5.
- [47] He K, Zhang X, Ren S, Sun J. Deep residual learning for image recognition. In: *Proceedings of the IEEE conference on computer vision and pattern recognition*; 2016. p. 770-8.
- [48] Su J, Ahmed M, Lu Y, Pan S, Bo W, Liu Y. RoFormer: Enhanced transformer with Rotary Position Embedding. *Neurocomputing*. 2024;568:127063. Available from: <https://www.sciencedirect.com/science/article/pii/S0925231223011864>.
- [49] Dao T. FlashAttention-2: Faster Attention with Better Parallelism and Work Partitioning. In: *International Conference on Learning Representations (ICLR)*; 2024. .
- [50] Shazeer N. GLU Variants Improve Transformer. *CoRR*. 2020;abs/2002.05202. Available from: <https://arxiv.org/abs/2002.05202>.
- [51] Loshchilov I, Hutter F. Decoupled Weight Decay Regularization. In: *International Conference on Learning Representations*; 2019. Available from: <https://openreview.net/forum?id=Bkg6RiCqY7>.
- [52] Tonami N, Imoto K, Okamoto Y, Fukumori T, Yamashita Y. Sound Event Detection Based on Curriculum Learning Considering Learning Difficulty of Events. *ICASSP 2021 - 2021 IEEE International Conference on Acoustics, Speech and Signal Processing (ICASSP)*. 2021:875-9. Available from: <https://api.semanticscholar.org/CorpusID:231861571>.
- [53] Paszke A, Gross S, Massa F, Lerer A, Bradbury J, Chanan G, et al. PyTorch: An Imperative Style, High-Performance Deep Learning Library. *CoRR*. 2019;abs/1912.01703. Available from: <http://arxiv.org/abs/1912.01703>.
- [54] Cañas JS, Toro-Gómez MP, Sugai LSM, et al. A dataset for benchmarking Neotropical anuran calls identification in passive acoustic monitoring. *Scientific Data*. 2023;10:771. Available from: <https://doi.org/10.1038/s41597-023-02666-2>.
- [55] Yoh N, Mbamy W, Gottesman BL, Froese GZL, Satchivi T, Obiang Ebanega M, et al. Impacts of logging, hunting, and conservation on vocalizing biodiversity in Gabon. *Biological Conservation*. 2024;296:110726. Available from: <https://www.sciencedirect.com/science/article/pii/S000632072400288X>.
- [56] Navine A, Kahl S, Tanimoto-Johnson A, Klinck H, Hart P. A collection of fully-annotated soundscape recordings from the Island of Hawai'i; 2022. Available from: <https://doi.org/10.5281/zenodo.7078499>.
- [57] Dufourq E, Durbach I, Hansford JP, Hoepfner A, Ma H, Bryant JV, et al. Automated detection of Hainan gibbon calls for passive acoustic monitoring. *Remote Sensing in Ecology and Conservation*. 2021;7(3):475-87. Available from: <https://zslpublications.onlinelibrary.wiley.com/doi/abs/10.1002/rse2.201>.

- [58] Allen AN, Harvey M, Harrell L, Jansen A, Merkens KP, Wall CC, et al. A Convolutional Neural Network for Automated Detection of Humpback Whale Song in a Diverse, Long-Term Passive Acoustic Dataset. *Frontiers in Marine Science*. 2021;8:607321.
- [59] Symes L, Madhusudhana S, Martinson S, et al.. Neotropical forest soundscapes with call identifications for katydids. *Dryad*; 2023. Dataset. Available from: <https://doi.org/10.5061/dryad.zw3r2288b>.
- [60] Zhang YJ, Huang JF, Gong N, Ling ZH, Hu Y. Automatic detection and classification of marmoset vocalizations using deep and recurrent neural networks. *The Journal of the Acoustical Society of America*. 2018;144(1):478. Available from: <https://pubmed.ncbi.nlm.nih.gov/30075670/>.
- [61] Chronister LM, Rhinehart TA, Place A, Kitzes J. An annotated set of audio recordings of Eastern North American birds containing frequency, time, and species information. *Ecology*. 2021;102(6):e03329. Available from: <https://esajournals.onlinelibrary.wiley.com/doi/abs/10.1002/ecy.3329>.
- [62] Lapp S, Larkin JL, Parker HA, Larkin JT, Shaffer DR, Tett C, et al. Automated recognition of ruffed grouse drumming in field recordings. *Wildlife Society Bulletin*. 2023;47(1):e1395. Available from: <https://wildlife.onlinelibrary.wiley.com/doi/abs/10.1002/wsb.1395>.
- [63] Lapp S, Smith TC, Knapp RA, Lindauer A, Kitzes J. Aquatic Soundscape Recordings Reveal Diverse Vocalizations and Nocturnal Activity of an Endangered Frog. *The American Naturalist*. 2024;203(5):618-27. PMID: 38635364. Available from: <https://doi.org/10.1086/729422>.
- [64] Simard Y, Roy N, Giard S, Aulancier F. North Atlantic right whale shift to the Gulf of St. Lawrence in 2015 as monitored by long-term passive acoustics. *Endangered Species Research*. 2019 12;40.
- [65] Hopcroft JE, Karp RM. An  $n^{5/2}$  algorithm for maximum matchings in bipartite graphs. *SIAM J Comput*. 1973;2(4).
- [66] Chen S, Wu Y, Wang C, Liu S, Tompkins D, Chen Z, et al. BEATs: audio pre-training with acoustic tokenizers. In: *Proceedings of the 40th International Conference on Machine Learning. ICML'23. JMLR.org*; 2023. .
- [67] Snell J, Swersky K, Zemel R. Prototypical networks for few-shot learning. *Advances in neural information processing systems*. 2017;30.
- [68] Stidsholt L, Johnson M, Beedholm K, Jakobsen L, Kugler K, Brinkløv S, et al. A 2.6-g sound and movement tag for studying the acoustic scene and kinematics of echolocating bats. *Methods in Ecology and Evolution*. 2019;10(1):48-58.
- [69] Symes LB, Madhusudhana S, Martinson SJ, Kernan CE, Hodge KB, Salisbury DP, et al.. Estimation of katydid calling activity from soundscape recordings.; 2022.
- [70] Sarkar E, Magimai Doss M. Can Self-Supervised Neural Representations Pre-Trained on Human Speech distinguish Animal Callers? In: *Proceedings of INTERSPEECH 2023*; 2023. p. 1189-93. Available from: [https://www.isca-archive.org/interspeech.2023/sarkar23\\_interspeech.pdf](https://www.isca-archive.org/interspeech.2023/sarkar23_interspeech.pdf).
- [71] Kirsebom OS, Frazao F, Simard Y, Roy N, Matwin S, Giard S. Performance of a deep neural network at detecting North Atlantic right whale upcalls. *The Journal of the Acoustical Society of America*. 2020;147(4):2636-46.
- [72] Traer J, McDermott JH. Statistics of natural reverberation enable perceptual separation of sound and space. *Proceedings of the National Academy of Sciences*. 2016;113(48):E7856-65. Available from: <https://www.pnas.org/doi/abs/10.1073/pnas.1612524113>.



## A FASD13 Summary

For all datasets, if there were overlapping bounding boxes corresponding to multiple events, we merged these bounding boxes into a single bounding box.

**Anuraset:** Subset of twelve recordings from the strongly-labeled portion of AnuraSet [54]. The original study collected soundscape recordings from omni-directional microphones placed near four bodies of water in Brazil. The dataset was developed to improve automated classification of anuran vocalizations. Expert annotators identified the start- and end-times of vocalizations, for each of 42 different frog species. For our purpose, four recordings were selected for each of three frog species (*Boana lundii*, *Leptodactylus latrans*, *Physalaemus albonotatus*); annotations in these recordings that corresponded to other species were discarded.

**Carrion Crow:** Set of ten hour-long recordings of carrion crows (*Corvus corone*) near León, Spain. Recordings were made using on-body recorders [68] attached to the tails of adult crows. Recordings were made through a study investigating communication and cooperative behavior in groups of crows. One expert annotator identified the start- and end-times of vocalizations of adult crows and socially-parasitic great spotted cuckoo (*Clamator glandarius*) chicks. For our purpose, five recordings were selected for each species; annotations in these recordings that corresponded to the other species were discarded. Vocalizations by crow chicks, such as begging calls, are considered as background sound. Crow vocalizations were marked as “Unknown” when it was difficult to discern the life stage of the vocalizing individual.

**Gibbon:** Set of nine recordings from the Test split in [57]. Soundscape recordings were made in Hainan, China, using omni-directional microphones. The dataset was developed to improve monitoring of Hainan Gibbons (*Nomascus hainanus*), a critically endangered primate species. Expert annotators identified gibbon vocalizations, and annotated start- and end-times up to the closest second.

**Gunshot:** Set of recordings from seven sites, taken from the Test split of the gunshot detection dataset presented in [55]. Recordings were made in forests in Gabon, using omni-directional microphones. The dataset was developed to investigate impacts of hunting on biodiversity in Gabon. Annotators marked the start- and end-times of gunshots. For our purpose, we collated all recordings from a single site into a single recording. Then, we discarded recordings which had fewer than seven detected gunshots.

**Hawaiian Birds:** Subset of twelve recordings from the dataset presented in [56]. Recordings were made at a variety of locations in Hawaii, using omni-directional microphones. The recordings were collected for a variety of studies conducted by the Listening Observatory for Hawaiian Ecosystems at the University of Hawai‘i at Hilo. Expert annotators were asked to draw a spectrogram bounding box around each vocalization of 27 bird species present in Hawaii. Vocalizations separated by less than 0.5 seconds were allowed to be included in a single bounding box. For our purpose, four recordings were selected for each of three bird species (*Chlorodrepanis virens*, *Myadestes obscurus*, *Pterodroma sandwichensis*); annotations in these recordings that corresponded to other species were discarded.

**Humpback** Subset of ten hour-long recordings from the dataset presented in [58]. Recordings were collected at sites in the North Pacific by bottom-mounted, omni-directional hydrophones. The dataset was developed to train a humpback whale (*Megaptera novaeangliae*) vocalization detector. We considered the “initial” audit portion of the data from this publication, in which experts annotated full recordings for humpback whale vocalizations and un-annotated time periods implicitly do not contain whale vocalizations. For our purpose, we selected ten recordings. The recordings were divided into 75-second chunks, and for each recording we discarded all subchunks which did not contain at least one whale vocalization.

**Katydid** Subset of twelve recordings from the dataset presented in [59, 69]. Recordings were made in the forest canopy of Barro Colorado Island in Panamá, using an omni-directional microphone. The dataset was developed to quantify the calling activity of katydids (*Tettigoniidae*). Expert annotators identified the start- and end-times of katydid calls, for 24 species of katydids. For our purpose, we selected four recordings for each of three katydid species (*Anaulacomera darwinii*, *Thamnobates subfalcata*, *Pristonotus tuberosus*); annotations in these recordings that

corresponded to other species were discarded. Additionally, following the original study, we only retained annotations where the annotators were able to identify a clear pulse structure.

**Marmoset** Subset of ten recordings from the dataset presented in [70, 60]. Ten juvenile common marmosets (*Callithrix jacchus*) were each placed in a sound-proofed room, away from other individuals, and their spontaneous vocalizations were recorded using a cardioid microphone. The dataset was developed in order to investigate the use of deep learning for detecting and classifying marmoset vocalizations. Annotators identified the start- and end-time of each vocalization, and categorized each vocalization according to one of ten pre-defined call types. For our purpose, we selected one ten-minute recording from each individual. In five of these recordings, we retained annotations corresponding to the “Phee” call; in the other five recordings we retained annotations corresponding to the “Twitter” call. Similar call types (“Peep”, “Trillphee”, “Pheecry”, “TrillTwitter”, “PheeTwitter”) were re-labeled as “Unknown”, and the remaining annotated call types were discarded.

**Powdermill** Recordings from the dataset presented in [61]. Four dawn chorus soundscapes were captured using omni-directional microphones at the Powdermill Nature Reserve, Pennsylvania, USA. The dataset was developed in order to provide a resource for research into automated bird sound classification and detection in soundscape recordings. Expert annotators marked the start- and end-times of vocalizations from 48 bird species. For our purpose, in two recordings we retained annotations of one bird species (Eastern Towhee, *Pipilo erythrophthalmus*), and in the other two recordings we retained annotations of a second bird species (Common Yellowthroat, *Geothlypis trichas*).

**Rana Sierrae** Subset of recordings from the dataset presented in [63]. Underwater soundscapes were captured using omni-directional microphones placed in waterproof cases that were attached to the bottom of a lake in California’s Sierra Nevada mountains. The data were collected to characterize the vocal activity of a wild population of the endangered Sierra Nevada yellow-legged frog (*Rana sierrae*). For each vocalization, annotators marked its start- and stop-time, and classified it into one of five call types. For our purposes, we concatenated all recordings from each single day presented in the original dataset. This yielded seven recordings, corresponding to the seven days of recording. For four recordings, we retained annotations of one call type, “Primary vocalization”, and for the other three recordings, we retained annotations of the other call types “Frequency-modulated call”.

**Right Whale** Subset of ten recordings from the dataset B\* presented in [71, 64]. Underwater soundscapes were recorded by hydrophones moored 5-50 meters above the bottom of the seafloor. The data were originally recorded as part of a study [64] documenting changes in the distribution of the endangered North Atlantic right whale (*Eubalaena glacialis*, NARW). Expert annotators manually midpoints of NARW upcalls. For our purpose, we extended each midpoint to a 1-second bounding box. The duration of this box was chosen based on the description of the NARW upcall in [71] as a “1-s, 100–200 Hz chirp with a 610 Hz bandwidth.”

**Ruffed Grouse** Recordings from the dataset presented in [62]. Recordings were made using omni-directional microphones placed in regenerating timber harvests in Pennsylvania, USA. The dataset was developed to evaluate the performance of an automated method to detect ruffed grouse (*Bonasa umbellus*) drumming events. In the original study, five-minute clips were extracted from the original recordings, and annotators marked the start- and end-times of each drumming event. For our purpose, for each of the two months in the recording period (April and May, 2020), we concatenated all the recordings into a single audio file.

**Spider** Four recordings provided by the Damian Elias lab. Male jumping spiders (*Habronattus* species) perform solid-borne acoustic displays in mating contexts. These displays were recorded using a laser vibrometer directed at the substrate on which spiders were standing. The dataset was collected as part of a study investigating signal evolution across the genus. Expert annotators labeled the start- and end-times of each spider signal, along with a signal-type category from a pre-defined list. For our purposes, for two files we retained labels signals labeled “thumping”; for the other two files we retained labels from signals labeled “knocking”.

## B Data Generation Parameters

**Sampling** For sampling target pseudovox, an event rate  $r$  is drawn from  $\{1, 0.5, 0.25, 0.125, 0.0625\}$  events per second. The number  $n$  of pseudovox that will appear in a  $\text{dur}$ -second scene is drawn from a Poisson distribution with rate parameter  $r \times \text{dur}$ . To reduce the number of event-less scenes, we set  $n = \max(n, 1)$  with probability 1 for support scenes and with probability 0.5 for query scenes. A clustering level  $k$  is drawn from  $k \in K = \{\lfloor M/128 \rfloor, \lfloor M/64 \rfloor, \lfloor M/32 \rfloor, \lfloor M/16 \rfloor, \lfloor M/8 \rfloor\}$ , where  $M$  is the total number of pseudovox. A cluster is drawn at random from the  $k$ -means clustering of the pseudovox at this level, and  $n$  pseudovox are drawn from this cluster. This process is repeated for distractor pseudovox.

For background audio, two background tracks are sampled, looped to the scene duration, and overlaid. When constructing support-query pairs, for the query scene these background tracks are different from the support scene background tracks with probability  $p_{gen} = 0.5$

**Augmentation** With probability 0.2, all target pseudovox are flipped in time. To apply pitch/time shifting, a resampling rate  $\rho$  is drawn from  $\{0.3, 0.5, 0.7, 1, 1, 1, 1.5, 2\}$  and all target pseudovox are resampled from  $16k\text{Hz}$  to  $\rho \times 16k\text{Hz}$ . For amplitude augmentation, to simulate one or more individuals making sounds at different amplitudes, we construct a random Gaussian mixture model (GMM) with two components. Each component has a mean amplitude  $\mu_a \sim \text{Unif}(-12, 7)$  dB and a standard deviation  $\sigma_a \sim \text{Unif}(0, 5)$  dB. The weight of the second mixture component is drawn from  $\{0, 0, 0, 0, 0, 0.1, 0.2, 0.3, 0.4, 0.5\}$ . The SNR of each target pseudovox is set based on draws from this GMM and set based on the RMS amplitude of the background audio and pseudovox. To add reverb, we convolve with a recorded room impulse response drawn from [72]. This process is repeated for distractor pseudovox. We apply only resampling augmentations to background audio.

**Combination** To simulate one or more individuals making sounds at different rates, we construct a random GMM with two components that are used to sample time gaps between events in a scene. Each component has a mean  $\mu_t \sim \text{Unif}(0, 30)$  seconds and a standard deviation  $\sigma_t \sim \text{Unif}(0, 10)$  seconds. The weight of the second mixture component is drawn from  $\{0, 0, 0, 0, 0, 0.1, 0.2, 0.3, 0.4, 0.5\}$ . Target pseudovox are added to the background audio, one-by-one, with timegaps between consecutive events sampled from this GMM. Events that extend past the duration of the scene are looped back to the beginning. This process is repeated for distractor pseudovox.

**Variations for additional experiments** High homogeneity in events: Set cluster level  $k = \lfloor M/8 \rfloor$ . Low homogeneity in events: Set cluster level  $k = \lfloor M/128 \rfloor$ . High events / second: Set rate  $r = 1$  event per second Low events / second: Set rate  $r = 0.0625$  events per second Only high SNR events: SNR mean  $\mu_a$  is drawn from  $\text{Unif}(2, 7)$  dB. Only high SNR events: SNR mean  $\mu_a$  is drawn from  $\text{Unif}(-12, -7)$  dB.

## C Results on validation datasets

**Table 4: F1 scores @0.3 IoU on validation datasets.** Models marked with † were pre-trained using our generated data, rather than the data used in the original publication.

5-shot, within-recording							
Model	HB	ME	PB	PB24	PW	RD	Avg
Frozen Encoder + Linear	<b>.839</b>	.310	.067	.104	.668	.159	.358
Protonet	.788	.597	.321	.492	.211	.359	.461
Protonet <sup>†</sup>	.775	.518	.480	.482	.165	.335	.459
Transductive	.500	.173	.210	.342	.085	.143	.242
SCL	.719	.691	.538	.688	.080	.368	.514
SCL+finetuning	.779	.634	.577	.713	.077	.371	.525
SCL <sup>†</sup>	.578	.429	.374	.674	.090	.498	.440
SCL <sup>†</sup> +finetuning	.749	.486	.379	.659	.094	.353	.453
DRASDIC † (ours)	.659	<b>.829</b>	<b>.657</b>	<b>.809</b>	<b>.738</b>	<b>.532</b>	<b>.704</b>
0-shot							
Model	HB	ME	PB	PB24	PW	RD	Avg
BLED	<b>.081</b>	<b>.469</b>	.238	<b>.588</b>	.009	.458	<b>.307</b>
DRASDØS † (ours)	.000	.134	<b>.424</b>	.560	<b>.070</b>	<b>.531</b>	.287

## D FASD13 visualizations

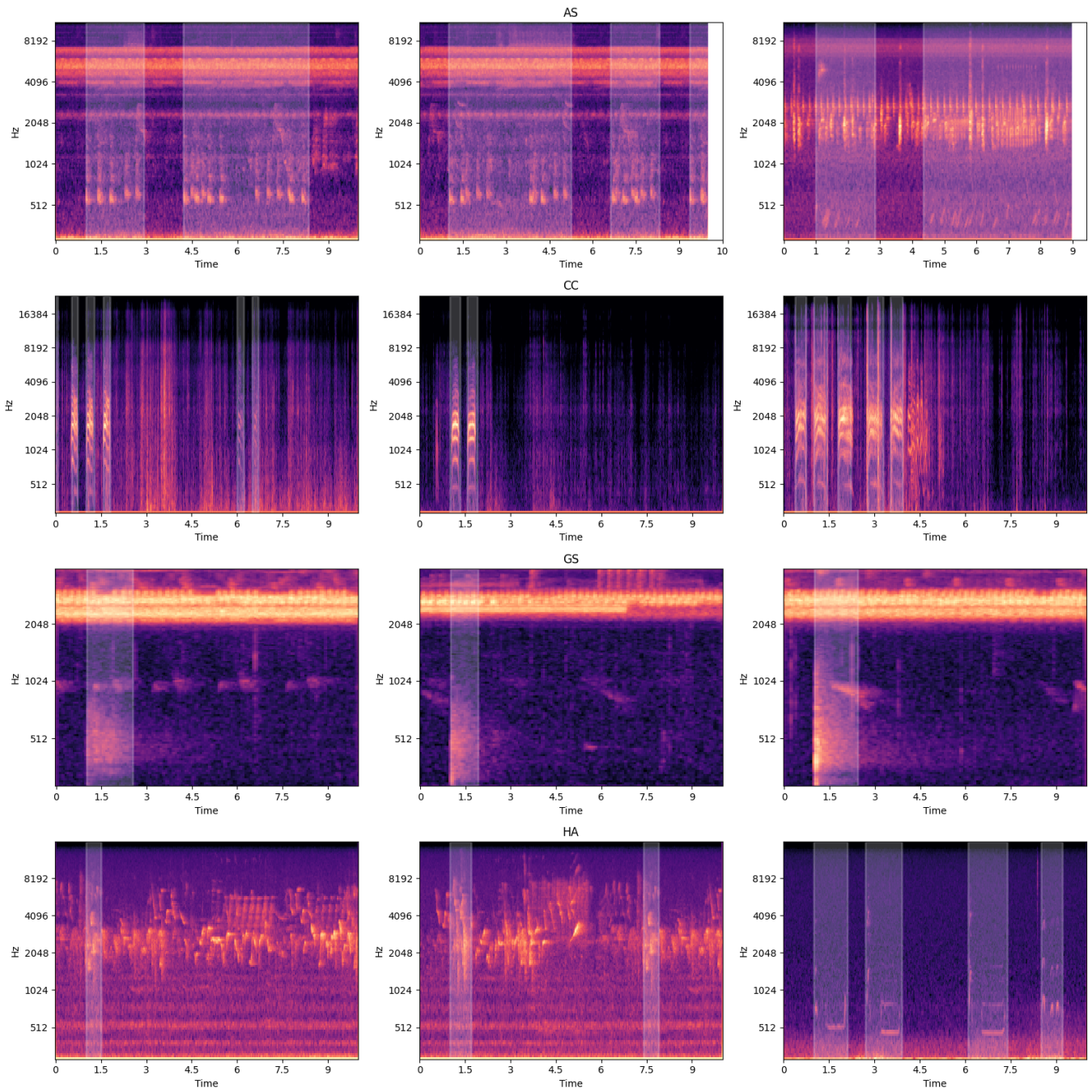


**Figure 5:** Example spectrograms from FASD13, part 1. Each row contains three spectrograms from one dataset. Positive events are highlighted.



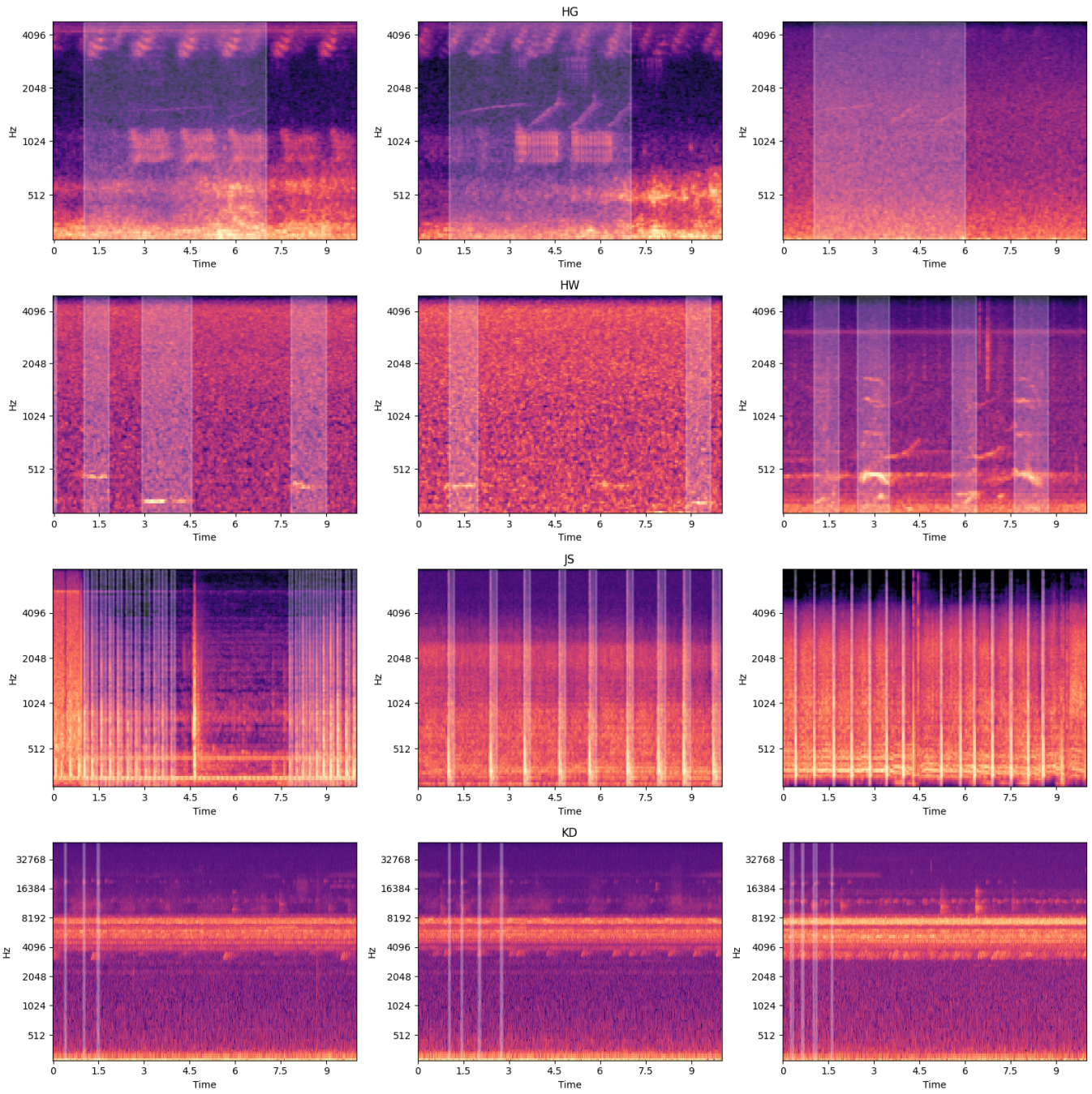


**Figure 6:** Example spectrograms from FASD13, part 2. Each row contains three spectrograms from one dataset. Positive events are highlighted.



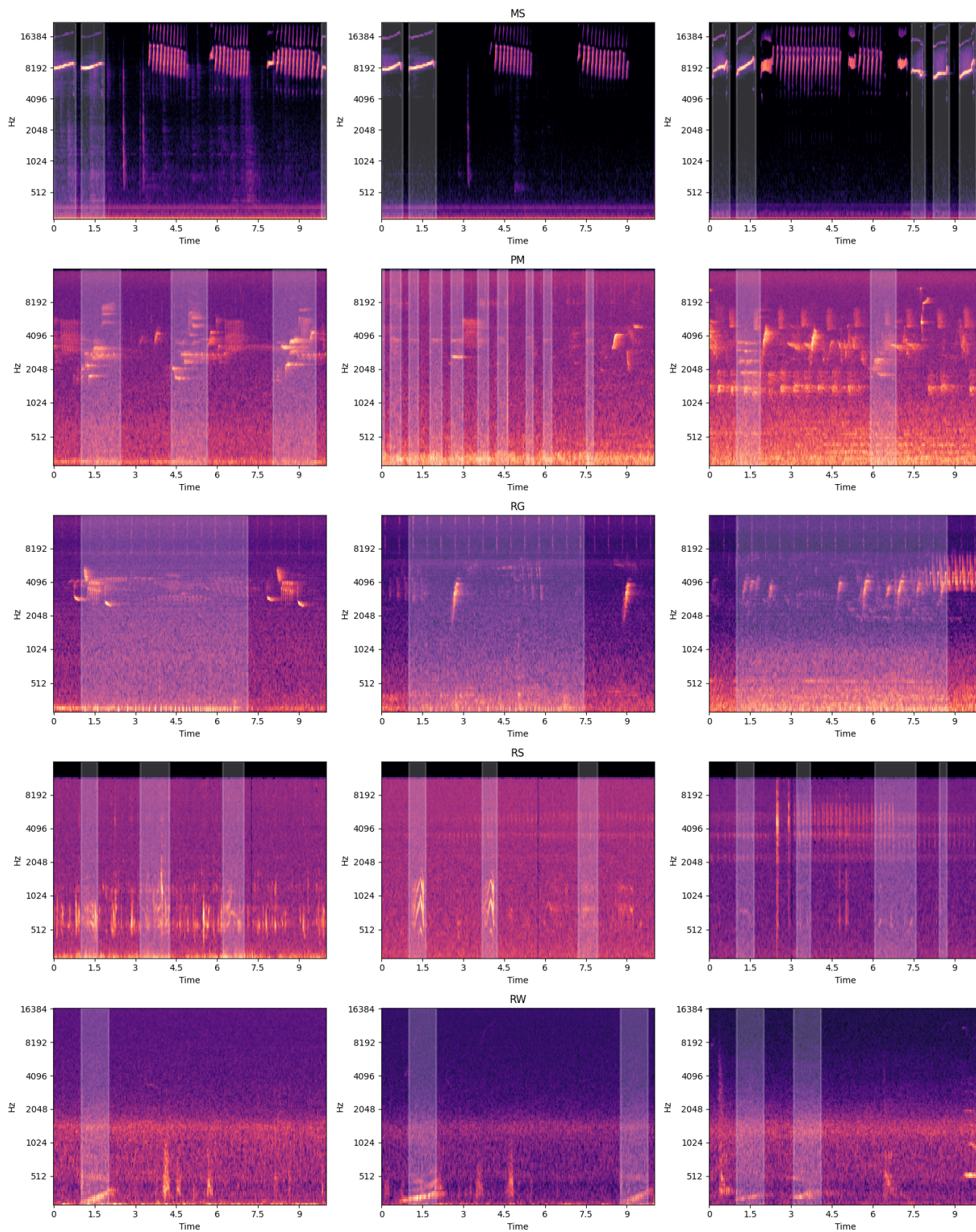


**Figure 7:** Example spectrograms from FASD13, part 3. Each row contains three spectrograms from one dataset. Positive events are highlighted.

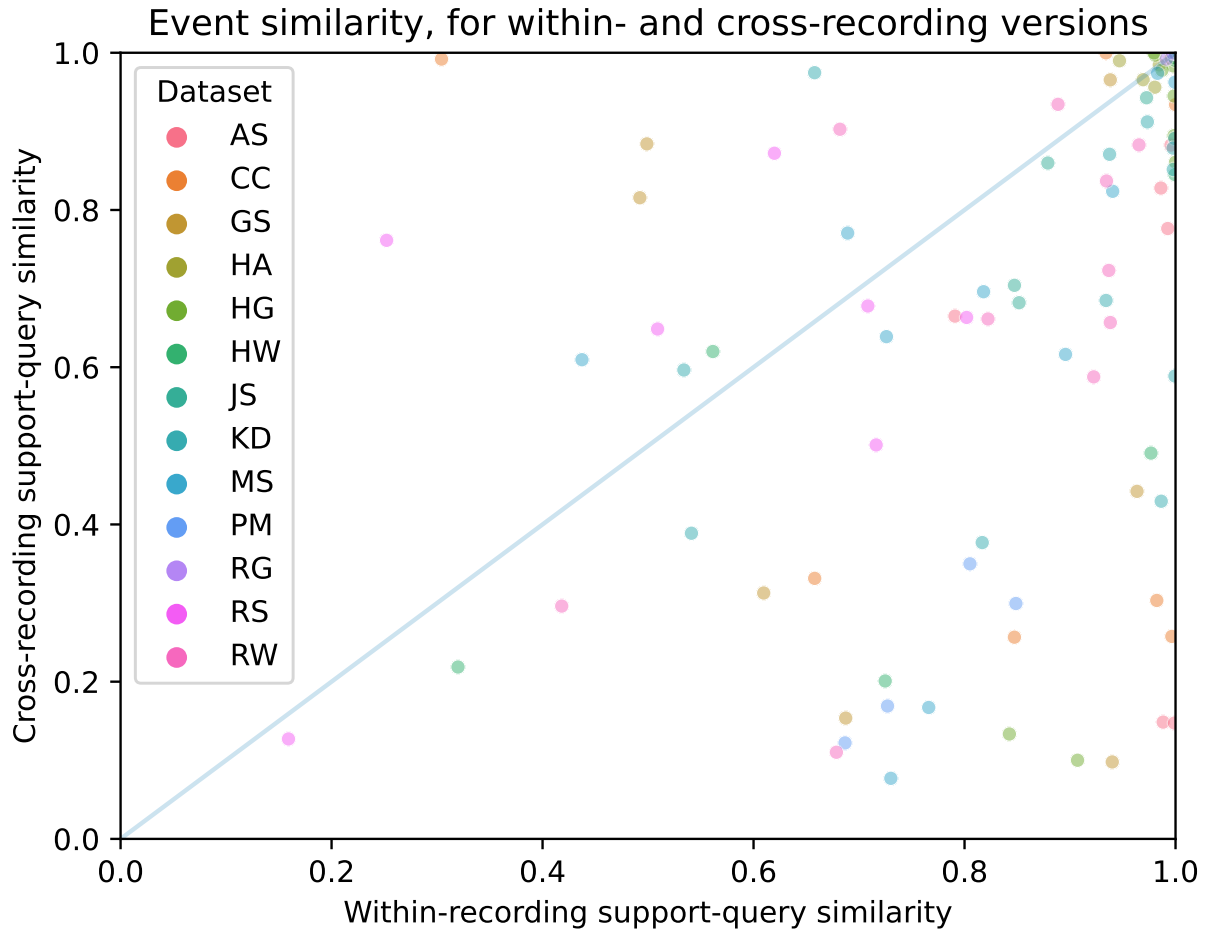


**Figure 8:** Comparison of within- and cross-recording versions. For each support set, we computed the mean power mel-spectrum of A) the foreground (event) audio of the support set, B) the foreground audio of the within-recording query set, and C) the foreground audio of the cross-recording query set. The cosine similarity of A) and B) is on the horizontal axis, and of A) and C) on the vertical axis. 79% of support foreground audio is more similar to the within-recording query audio (i.e. below the line of slope=1) than to the cross-recording query audio. A similar trend holds for background audio: 69% of support background audio is more similar to the within-recording query audio than to the cross-recording query audio.